

# Computerized Buckling Models for Ultimate Strength Assessment of Stiffened Ship Hull Panels

Eivind Steen<sup>1)</sup>, Eirik Byklum<sup>1)</sup>, Kjetil G. Vilming<sup>1)</sup> and Tom K. Østvold<sup>1)</sup>

<sup>1)</sup> Technical Consultancy Services, Det Norske Veritas.  
Høvik, Norway

## Abstract

Direct application of geometrical non-linear plate theory is the main concept in the new Panel Ultimate Limit State (PULS) stiffened panel models recently recognized by Det Norske Veritas as part of the new rules and standards for ships and offshore constructions. The focus is on assessment of the ultimate capacity limit, rather than the more traditional elastic buckling limit. The method is streamlined for rules based on modern ultimate limit state design principles. The models are validated against non-linear FE analyses and laboratory experiments. Comparison against existing codes used by Classification Societies are included.

## Keywords

Strength; Buckling; Postbuckling; Ultimate strength; Stiffened panels; Non-linear; Combined loads.

## Introduction

Stiffened panels is the main structural building block in ship hulls, and their structural response under compressive loading is a topic of significant practical interest in ship design. This applies for the detail design phase as well as for ships in the service phase for which a trustworthy strength and safety margin assessment are of paramount importance.

It is well known that postbuckling and ultimate strength limits only can be treated in a consistent manner using non-linear plate theory. This fact has for many decades been an obstacle for practising engineers and designers since resort to advanced and time consuming non-linear finite element programs and expert judgements were a prerequisite for assessing the strength of critical elements. However, with the recent development of computers, it has become feasible to make use of buckling models based on non-linear plate theory.

By introducing semi-analytical computerized ultimate strength models into ship and offshore rules and standards, engineers and designers will improve their understanding of non-linear structural response. The result

will be more optimal and robust design solutions with more effective use of the material and improved control of the actual safety margins against failure. Corrosion margins and minimum thickness requirements for ships in service can be prescribed with larger confidence than hitherto possible with simpler and more traditional curve fitting methods.

This paper gives a brief description of the background for the stiffened panel models used in PULS, and comparison against non-linear FE analysis, laboratory tests, and Classification Societies Rules.

## Description

The PULS buckling code is developed for direct computational assessment of buckling limits and ultimate strength limits of stiffened panels. The idea is to combine a user friendly and easy to understand user interface, with advanced but still efficient direct calculations. The numerical algorithms included in the buckling code provide results for a given case in the order of a second on a standard modern personal computer.

There are currently three different buckling models developed for the PULS code. The unstiffened plate model is illustrated in Figure 1, the regularly stiffened plate model is illustrated in Figure 2, and the non-regular geometry model is illustrated in Figure 3.

The regularly stiffened plate model is the one considered most relevant for stiffened panels in ship type structures, and the one described in this paper.

The unstiffened plate model is for plates where the edges are known to have rigid support in the lateral direction, and should therefore normally not be used for plate fields between stiffeners, since the stiffener deflection then is disregarded.

The plate model developed for non-regular geometry is based on linear plate theory. Hence, it is useful for areas of a ship hull with complex geometry, but it does not account for the non-linear postbuckling capacity of the panels.

All three models cover load combinations such as biaxial compression/tension, in-plane shear and lateral pressure loads as typical for panels in ship deck, bot-

toms, sides etc. Linearly varying stress perpendicular to the stiffener direction may also be considered.

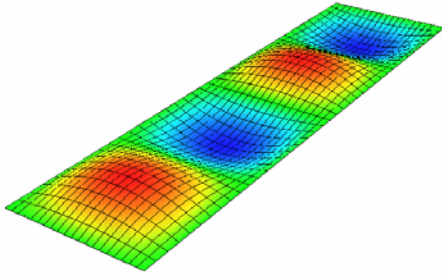


**Figure 1: PULS unstiffened plate model**

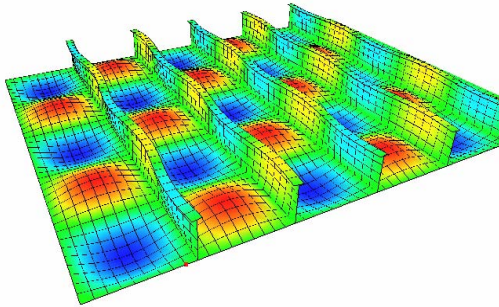


**Figure 2: PULS regularly stiffened plate model**

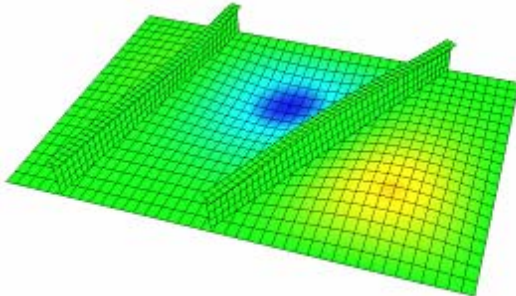


**Figure 3: PULS non-regular geometry model**

## Theory

### General principles

The PULS buckling models can be classified as semi-analytical in the sense that they are based on the recognized plate theory of Marguerre (1938) in combination with numerical techniques for solution of the governing equations. Using non-linear plate theory, second order membrane strains are accounted for, and the postbuckling response may be traced.

The principle of minimum potential energy is used, together with Fourier series expansion of the displacements. The non-linear elastic equilibrium equations are

solved, and the load-deflection path traced, using the perturbation technique in an incremental scheme with arc length control. Using arc length incrementation, complex response histories may be solved, including snap-through problems.

The calculation procedure for the stiffened panel element can be split into three levels:

i) Local level: A non-linear analysis of the local buckling deflections is carried out, in order to determine the redistributed membrane stress pattern, as well as the orthotropic macro material coefficients. The macro material coefficients are reduced due to local plate and stiffener buckling as compared to classical linear elastic smeared coefficients.

ii) Global level: A non-linear analysis of the global buckling deflections is carried out, by use of the orthotropic macro material coefficients calculated on the local level.

iii) Ultimate limit state: Stress control is performed, incorporating the results from the local and the global analyses, with explicit solution of different limit state functions for identifying the most critical hot spot stress location along edges and stiffener plate connections.

The basic theoretical concepts were first described in Steen, Østvold, Valsgård (2001) using an orthotropic plate theory for describing the overall stiffened panel response and using reduced macro coefficients for coping with the interaction between overall and local buckling in the panel. The local and the overall models were subsequently improved using advanced multiple degree of freedom models. Byklum and Amdahl (2002A), Byklum and Amdahl (2002B), and Byklum (2002C) describe details of the local model. Byklum, Steen and Amdahl (2003) gives details on the overall model. Some features and examples are also documented in Steen, Byklum, Vilming (2004).

### Local buckling model

The local buckling model is developed based on the assumption that the intersection between the plate and the stiffener does not deflect in the lateral direction. The edges of the plate are assumed to be free to move in-plane, but forced to remain straight. This restriction is imposed due to the effect of the neighboring plates that support the plate in a larger structure. The additional and initial deflections are taken as a Fourier series. The initial deflection represents the out-of-plane imperfection resulting from the fabrication process. The displacement function for the local deflection is taken as

$$w_1(x, y) = \sum_{m=1}^{M_s} \sum_{n=1}^{N_s} A_{mn}^s \sin\left(\frac{m\pi x}{a}\right) \sin\left(\frac{n\pi y}{b}\right) \quad (1)$$

where  $a$  is plate length, and  $b$  plate width. The initial deflection is similar. No assumptions are made regarding the deflection amplitudes. The deflection shape adjusts itself to the one which minimizes the total energy of the system, depending on the plate geometry and loading. The displacement shape chosen for the sideways deflection of the stiffener consists of a rigid tor-

sion part and a web bending part

$$v(x) = \frac{z}{h} \sum_{m=1}^{M_s} V_{1m} \sin\left(\frac{m\pi x}{a}\right) + (1 - \cos\left(\frac{\pi z}{2h}\right)) \sum_{m=1}^{M_c} V_{2m} \sin\left(\frac{m\pi y}{a}\right) \quad (2)$$

where  $h$  is the stiffener web height. The initial stiffener deflection is similar. Restrictions on the stiffener deflection are imposed by requiring continuity of rotation between the plate and the stiffener web

$$\left. \frac{\partial v}{\partial z} \right|_{z=0} = - \left. \frac{\partial w}{\partial y} \right|_{y=0} \quad (3)$$

Longitudinal continuity is ensured by requiring equal displacement in the longitudinal direction for the plate and the stiffener.

Having computed all strain components in the plate and the stiffener, the potential energy is calculated by analytical integration over the plate and stiffener volume. Closed form expressions are obtained for all contributions. Using an incremental form of the principle of minimum potential energy, the nonlinear response is traced in the solution space by using small incremental steps for the arc length parameter along the equilibrium path. For each increment in the local analysis, displacements and stresses are calculated, as well as the reduction in in-plane and out-of-plane stiffness due to the deflections. This macro stiffness reduction is used as input to the global buckling analysis, while the stress distribution is used for stress control in the ultimate limit state assessment.

### Global buckling model

In the global buckling model, the panel is considered as an equivalent orthotropic plate. The linear orthotropic stiffness coefficients are reduced to the local deflections, determined from the local analysis.

Two stiffener spans are considered in the global model, in order to account for the clamping-effect from lateral pressure. The displacement function is taken as a combination of the clamped mode and a simply supported mode

$$w_g(x, y) = \sum_{m=1}^{M_s} \sum_{n=1}^{N_s} A_{mn}^s \sin\left(\frac{m\pi x}{a}\right) \sin\left(\frac{n\pi y}{B}\right) + \sum_{m=1}^{M_c} \sum_{n=1}^{N_c} \frac{A_{mn}^c}{2} (1 - \cos\left(\frac{2m\pi x}{a}\right)) \sin\left(\frac{n\pi y}{B}\right) \quad (4)$$

where  $B$  is the total panel width.

As for the local model, the potential energy is calculated by analytical integration over the panel volume, and the nonlinear response is traced by solving the equilibrium equations in incremental steps. For each increment in the local analysis, displacements and bending stresses are calculated, for use in stress control in the ultimate limit state assessment.

### Capacity assessment

The capacity assessment is based on the principle that elastic local buckling is acceptable, but permanent deflections or global buckling of the panel should not take place. Hence, the ultimate strength value is found by considering the redistributed membrane stress pattern, and ensuring that the von Mises stress in certain critical positions stays below the onset of yielding. Since the analysis is terminated at the onset of yielding, spread of plasticity is not considered.

Global buckling is avoided by limiting the ultimate capacity to never exceed the global elastic buckling limit.

### Result presentation

For each load combination analysed, utilization factors with respect to ultimate capacity and elastic buckling is calculated. The utilization factors are determined by scaling the loads proportionally up until collapse is reached. The utilization factor is then the ratio of the applied loads to the ultimate loads. Elastic buckling limits (eigenvalues) are given for the local buckling and the global buckling. The elastic buckling limits may be of interest in case of functional requirements. In addition, information about the most critical position in the panel is given, as well as macro stiffness coefficients of the panel due to the local deflections.

Graphical results are available in the form of three-dimensional deflection plots showing eigenmodes, imperfections, and ultimate capacity deflection. Stress plots showing the redistributed membrane stress due to the buckling deflections are also included. An example is given in Figure 4, which shows the redistributed membrane stress in the axial direction, for a panel subjected to axial load. It is believed that this type of additional information contributes to an improved understanding of the buckling problem.

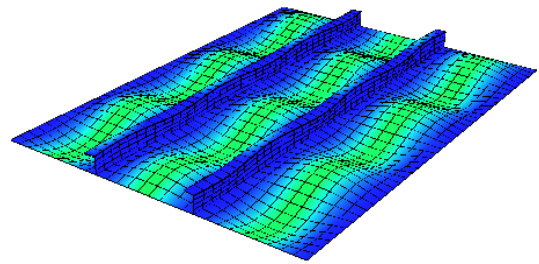


Figure 4: Redistributed axial membrane stress

Capacity interaction curves in load space may be generated for any of the combinations  $(\sigma_1, \sigma_2)$ ,  $(\sigma_1, \tau_{12})$ , and  $(\sigma_2, \tau_{12})$ . For each combination, a fixed pre-stress in the third stress component may also be specified, as well as a fixed lateral pressure component. A typical example of biaxial,  $(\sigma_1, \sigma_2)$ , capacity curves, for various levels of shear stress  $\tau_{12}$  is shown in Figure 5.

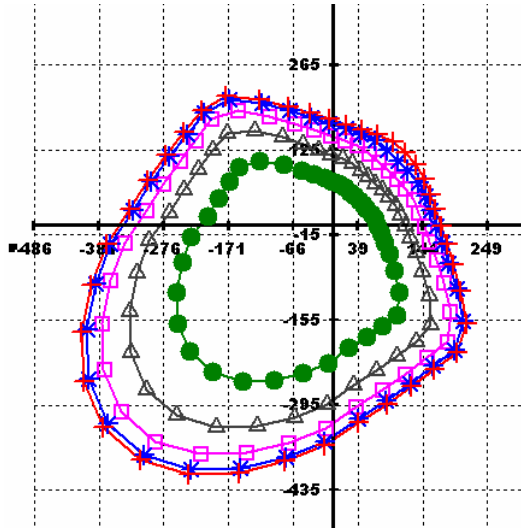


Figure 5: Biaxial capacity curve “slices”, for various levels of shear stress

Each point in the capacity curves is generated by increasing a reference combined nominal stress level ( $\sigma_1$ ,  $\tau_{12}$ ) proportionally up to the ultimate load level ( $\sigma_{1u}$ ,  $\tau_{12u}$ ). In case of lateral pressure  $p$ , or a third in-plane prestress component, this loading is first increased up to the specified level and then kept fixed while the in-plane loads are increased proportionally up to collapse.

## Validation of method

### Validation by use of nonlinear finite element methods

A large number of nonlinear finite element analyses have been carried out using the commercial program ABAQUS. These are documented in the report Steen, Vilming and Byklum (2004A). A few cases are presented here.

It is believed that fully nonlinear finite element codes are able to predict buckling deflection and ultimate collapse of stiffened panel with an accuracy which is sufficient for practical purposes, provided that the analyses are carried out properly. Due attention must be given to issues such as boundary conditions, mesh size, model extent, element types, and imperfections.

All the finite element analyses are carried out by modelling three stiffener spans in the longitudinal direction, and the entire stiffened panel between two longitudinal girders in the transverse direction. Imperfections are applied to the finite element models in the same way as done in the PULS models, by combining local eigenmodes with a global imperfection mode.

Capacity curves for bi-axial compression of a bottom panel of a 173m tanker are presented in Figure 6. The panel parameters are  $L=2400\text{mm}$ ,  $s=800\text{mm}$ ,  $t_p=13.5\text{mm}$ ,  $\text{NoS}=6$ , bulb profiles,  $h=240\text{mm}$ ,  $t_w=11\text{mm}$ ,  $\sigma_F=355\text{MPa}$ . In addition to the capacity curves calculated using PULS and ABAQUS, the local elastic buckling (eigenvalues) values calculated by PULS are presented (denoted LEB in the figure). Re-

sults for the same panel under combined in-plane compression and lateral pressure are presented in Figure 7.

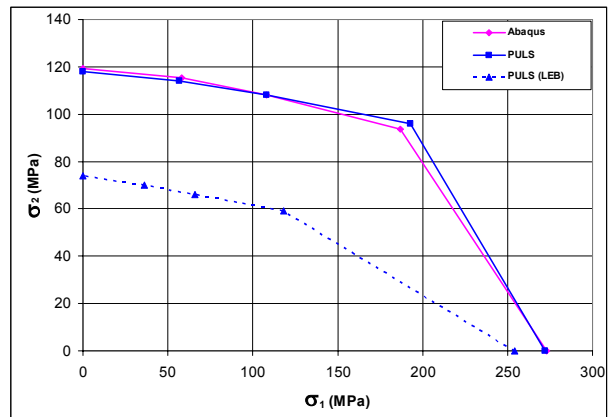


Figure 6: Tanker bottom panel, biaxial compression, without lateral pressure

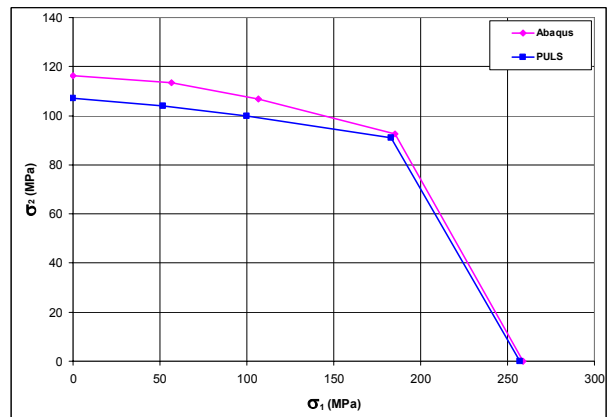


Figure 7: Tanker bottom panel, biaxial compression and lateral pressure on plate side  $p=151\text{ kN/m}^2$

The comparisons of ultimate strength capacities using ABAQUS and PULS are very consistent and within a  $\pm 10\%$  deviation for most cases. Such deviations are to be expected as the methods are very different. Typically the largest deviations are for regions in load space where the failure mode is not unique, i.e. in regions where mode interactions are strong and the program results rely heavily on how the geometrical imperfections are modelled - particularly with respect to shape, definition of boundary conditions and load history definition. The robustness of the numerical solution algorithm is also vital and of particular importance for load combination cases leading to mode interactions.

It is seen that the reduction in the in-plane capacity is not very much reduced when the design lateral pressure is applied. The reduction is somewhat larger for pure transverse compression for PULS than for ABAQUS.

It is also seen that the capacities predicted by both programs are far above the local elastic buckling values. This is typical for panels having a relatively small plate thickness. For such panels, the real ultimate capacity may be much higher than the buckling load. The additional capacity beyond elastic buckling varies signifi-

cantly depending on the load combination. The deflections of the panel at the ultimate limit state under pure axial load is shown in Figure 8.

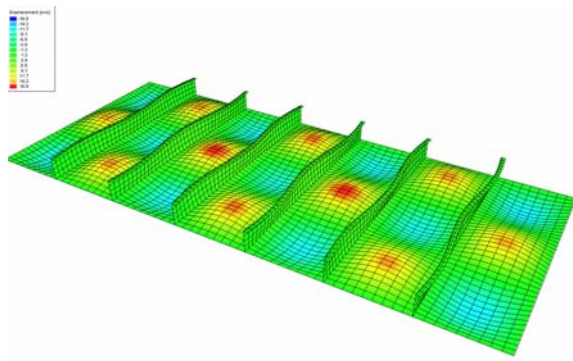


**Figure 8: Deflections at ULS under axial load for tanker bottom panel**

Capacity curves for combined shear load and transverse compression of a bulk carrier side panel are presented in Figure 9. Ship sides in bulk carriers are stiffened vertically by T or L profiles. The loading is typically compression perpendicular to the stiffener direction (transverse) acting simultaneously with in-plane shear and lateral pressure from the sea. The stiffener span can be very high and therefore an example with 8800 mm stiffener length and 890 mm stiffener spacing is presented here. The panel parameters are  $L=8800\text{mm}$ ,  $s=890\text{mm}$ ,  $t_p=14.5\text{mm}$ ,  $\text{NoS}=5$ , tee-bars,  $h=700\text{mm}$ ,  $t_w=13\text{mm}$ ,  $bf=150\text{mm}$ ,  $tf=18\text{mm}$ ,  $\sigma_F=355\text{MPa}$ . Results for the same panel under combined transverse compression, shear, and lateral pressure are presented in Figure 10.

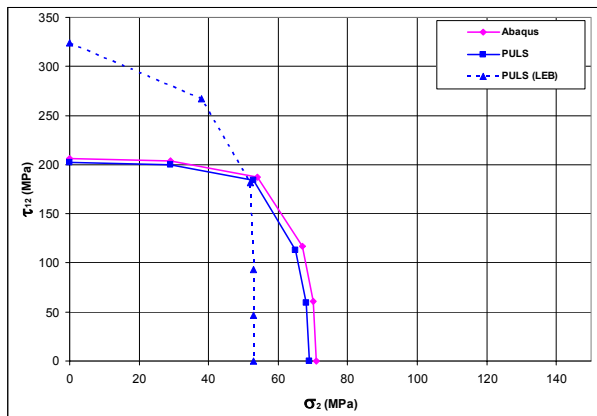


**Figure 9: Bulk carrier side panel, transverse compression and shear, without lateral pressure**

For pure shear loading, the strength is very close to the squash shear yield stress (shear yield stress =  $355/1.71 = 205\text{MPa}$ ) even though the elastic buckling stress (PULS LEB value) is not higher than  $\approx 320\text{MPa}$ , i.e. some 56 % in excess of the shear yield stress of  $205\text{MPa}$ . The main reason for this high shear strength is due to the significant postbuckling reserves beyond elastic buckling.

The strength for pure transverse loading is close to 70

MPa, which is significantly below squash yield stress of  $355\text{MPa}$ . This low ULS strength is indicated by the PULS LEB value which is as low as  $53\text{MPa}$  and by the reduced stiffness parameter  $C_{22}$  being as low as 40% measured relative to the linear-elastic full stiffness value. The latter parameter indicates a significant reduced transverse stiffness in the panel due to elastic buckling with a significant amount of redistribution of membrane stresses.

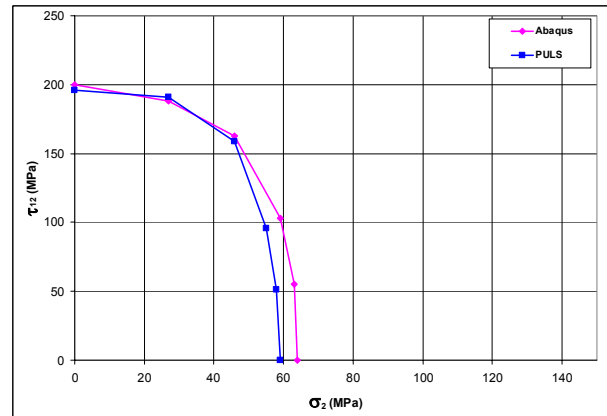


**Figure 10: Bulk carrier side panel, transverse compression, shear, and lateral pressure  $p=157\text{ kN/m}^2$**

This result is also easily verified by examining the ULS transverse stress distribution in the plate. This is shown in Figure 11, indicating a significant redistribution of membrane stresses from the mid regions in the plate towards the plate edges. The ABAQUS results are almost identical to the PULS results and confirm the relevance of the PULS theory.

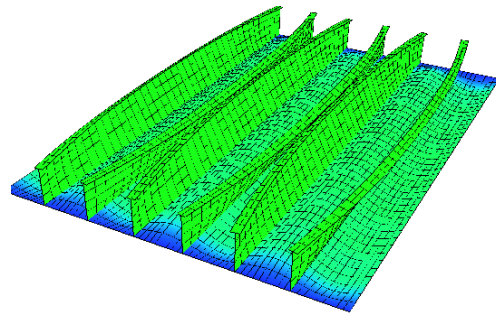


**Figure 11: Transverse membrane stress distribution at ULS for bulk side panel subjected to pure transverse compression, from PULS**

The presence of lateral pressure is not very important for the in-plane capacity of this panel, though more so for transverse dominated loading than for pure shear.

It can also be concluded that the PULS model shows very reasonable results as compared to the ABAQUS analyses covering load combinations dominated by yielding (shear) as well as load combinations dominated by elastic buckling (transverse compression). The comparisons are almost identical for the all the cases with-

out lateral pressure, while PULS are slightly on the conservative side for cases with fixed pressure of 0.157 MPa.

### Validation by use of results from experiments

Validation using experimental results is valuable, but few results are available in the literature for buckling of stiffened panels under combined in-plane loads. A series of experiments were carried out by Germanischer Lloyd in 1995 on panels subjected to combined biaxial compression and lateral pressure. A summary of the results was reported by Hayward (2003).

Capacity curves for bi-axial compression calculated by PULS for two of the GL test panels are presented in Figure 12 and Figure 13. Results are presented both for the case with lateral pressure and for the case without lateral pressure acting. The capacity obtained from the experiments are plotted as single points in the figures. The panel parameters for panel 1 are  $L=1320\text{mm}$ ,  $s=440\text{mm}$ ,  $t_p=6\text{mm}$ ,  $N_S=4$ , L profiles,  $h=80\text{mm}$ ,  $t_w=6\text{mm}$ ,  $b_f=20\text{mm}$ ,  $t_f=9.9\text{mm}$ ,  $\sigma_F=314\text{MPa}$  for the plate, and  $\sigma_F=292\text{MPa}$  for the stiffener. For panel 2,  $t_p=4\text{mm}$ ,  $\sigma_F=349\text{MPa}$  for the plate and  $\sigma_F=296\text{MPa}$  for the stiffener. The yield stresses were measured for each panel as part of the test, and the measured values were used in the PULS calculations. The imperfections used in PULS were the default values, but these are in the same range as the ones reported from the tests.

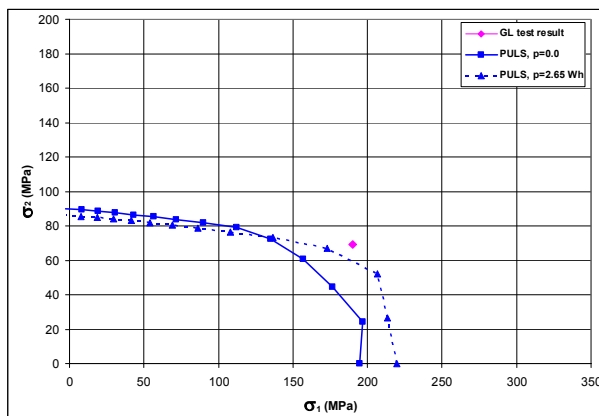


Figure 12: GL experimental model 1, biaxial compression and lateral pressure  $p=2.65\text{Wh}$

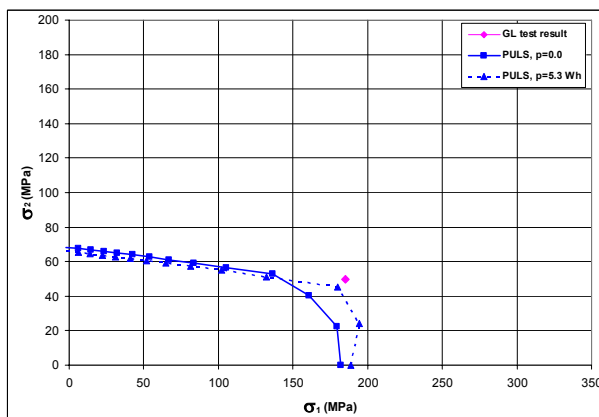


Figure 13 GL experimental model 2, biaxial compression and lateral pressure  $p=5.3\text{Wh}$

Both for panel 1 and panel 2, the PULS code predicts more strength for  $p=5.30\text{Wh}$  than with no pressure. This trend was qualitatively also shown in the GL tests, when comparing two similar panels subjected to different pressure magnitudes. However, GL has no tests with  $p=0$  for these panels so a direct quantitative comparison is not possible. The PULS results for the case with lateral pressure compare closely to the test results.

### Comparison with existing rules

It is relevant to see how the PULS code compares with existing ship rules for buckling. The DNV Ship Rules and the Germanischer Lloyd Rules for Seagoing Ships are chosen for comparison.

It is not straight-forward to compare different buckling codes. If different methods and assumptions are used, the results from two different codes may not be directly comparable.

One example is the concept of “usage factor”. In the PULS code, the capacity for each load combination is automatically calculated by increasing all loads proportionally until collapse, and the usage factor is given directly as the ratio of the applied loads divided by the capacity. This factor is not directly available from ordinary ship type rules, where various interaction equations are used. The left-hand-side in such interaction equations (required to be below or equal to 1.0) is not a real measure of the panel utilization. Hence, the only way to calculate the real utilization, is to find the factor that when multiplied with each load component gives a left-hand-side equal to 1.0. The usage factor for the applied loads is then the inverse of this factor.

It is also important to be aware of the cross-sectional area reference when comparing ultimate strength values in the form of stresses. The PULS code for stiffened panels (element S3) gives a nominal axial stress in the primary stiffener direction accounting for redistribution of stresses from plate mid-region towards the stiffeners and plate edges. The DNV rules and the GL rules, however, present the capacity as the nominal axial stress carried by the plating between the stiffeners only.

This fact is often missed among designers and this leads to confusion and misunderstandings when comparing different rules. The present comparison also neglects this difference since it is not possible to have a consistent measure of nominal stress in the ship rules and since this is the way designers would use the different rule approaches.

### Biaxial compression

Capacity curves for biaxial compression are presented for a tanker bottom panel in Figure 14. The panel is the same as the one considered in Figure 6, only now the results for the DNV Rules and the GL Rules are included. It is seen that PULS predicts more capacity than both of the rule formulations in the biaxial region. For pure axial compression, the DNV Rules seems to be overly conservative as compared with PULS and ABAQUS, while for pure transverse compression the GL Rules seems to be non-conservative. The GL Rules

interaction curve is close to linear, while the DNV Rules interaction curve is more convex, which is also the case for the PULS and ABAQUS curves.

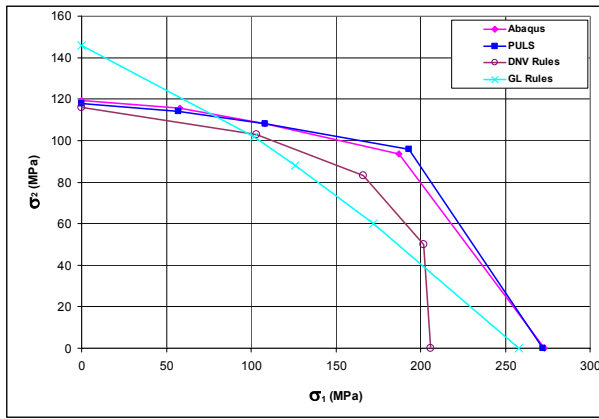


Figure 14: Tanker bottom panel subjected to biaxial compression

**Effect of shear load**

Capacity curves for combined shear load and transverse compression for a bulk carrier side panel are presented in Figure 15. The panel is the same as the one considered in Figure 9, only now the results for the DNV Rules and the GL Rules are included. It is seen that both of the rule formulations overpredict the capacity for pure transverse compression, while they significantly underestimate the capacity in the combined load region of the capacity curve.

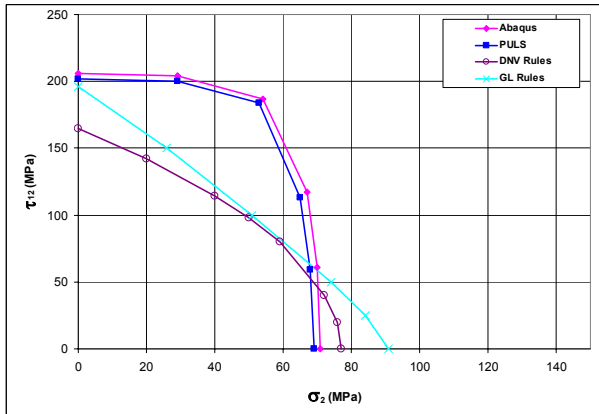


Figure 15: Bulk carrier side panel subjected to transverse compression and shear

Results for biaxial compression in combination with shear load is presented in Figure 16 for a bulk carrier bottom panel. The panel parameters are L=3680mm, s=875mm, tp=21mm, NoS=3, tee-bars, h=420mm, tw=9.6mm, bf=150mm, tf=17.6mm, sigma\_f=315MPa. The in-plane compression capacity is calculated for a fixed shear load of tau\_12=150MPa. It is seen that the biaxial capacity reduction due to the shear load is dramatic for both rule formulations, as compared with the PULS results. The difference between the two rule formula-

tions is also very large. This shows that it is very difficult to properly account for load combinations consisting of simultaneously acting axial load, transverse load, and shear by use of empirical interaction formulas. Finite element calculations have not been carried out for this case.

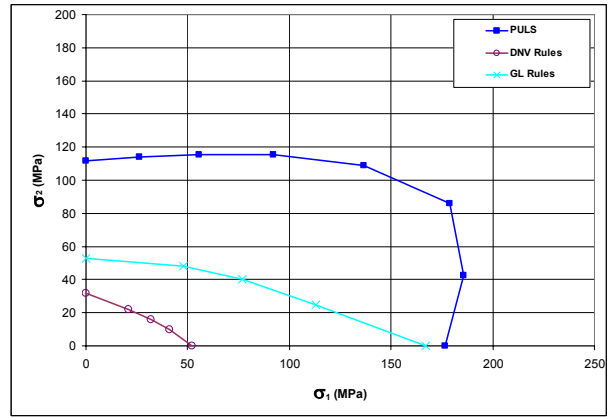


Figure 16: Bulk carrier bottom panel subjected to biaxial compression, with shear load tau\_12=150MPa

**Effect of lateral pressure**

In the DNV Rules, the in-plane capacity is not affected by the influence of lateral pressure, while for the GL Rules the pressure affects the lateral stiffener buckling only.

In Figure 17, the axial capacity for a tanker bottom panel is presented as a function of lateral pressure. The panel parameters are L=5120mm, s=910mm, tp=20mm, NoS=9, tee-bars, h=598.5mm, tw=12mm, bf=200mm, tf=20mm, sigma\_f=315MPa. It is seen that for large magnitudes of lateral pressure, the rule formulations overpredicts the capacity of the panel.

In Figure 18, the transverse capacity for the same panel is presented as a function of lateral pressure. It is seen that the transverse capacity is overpredicted in the rule formulations even for zero lateral pressure, and more so for increasing magnitude of pressure.

These examples show that lateral pressure does influence on the buckling capacity, and should be accounted for.

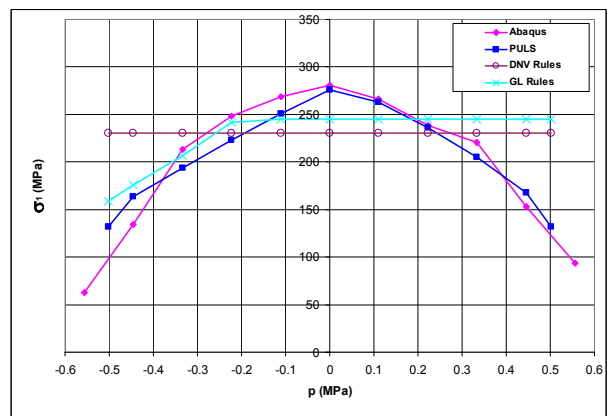
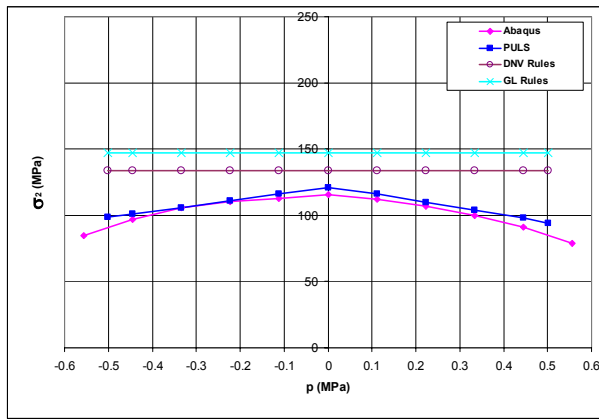


Figure 17: Effect of lateral pressure on axial capacity for tanker bottom panel



**Figure 18: Effect of lateral pressure on transverse capacity for tanker bottom panel**

### Observations

From the comparison between PULS, the DNV Rules and the GL Rules, it is observed that in general, higher capacity is predicted by the PULS code than by the ship rules. The ship rules are especially conservative in the biaxial region, for slender plates, and for shear loading. For slender plates, the capacity curves predicted by the GL Rules are close to linear, whereas the PULS curves and the DNV Rules are more convex. The GL Rules gives higher capacity for transverse loading for thick plates.

The DNV Rules do not account for the effect of lateral pressure, and may be non-conservative for larger magnitudes of pressure. For strong stiffeners, the GL rules has only effect of lateral pressure when acting on the stiffener side, and only for axial load. When the lateral pressure is acting on the plate side, the GL rules may be non-conservative. Also for lateral pressure and transverse load, the GL rules may be non-conservative.

### Conclusions

A direct calculation model for ultimate capacity assessment of stiffened panels has been developed, by use of energy principles and nonlinear plate theory. The direct calculation approach gives increased accuracy compared with conventional empirical based rules formulas. This is especially true for complex load combinations, and for non-standard geometries that the explicit design formulas were not originally created for. More information is also available in form of displacement shapes and redistributed stress patterns.

Validation of the method is performed by use of nonlinear finite element calculations and by comparison with available experimental data. Comparison is made with existing ship rules used by Classification Societies. It is found that the PULS code is generally consistent with results from nonlinear finite element calculations, as well as from laboratory tests.

The rules used by Classification Societies, however, is found to be conservative for some cases and non-

conservative for other cases, as compared with PULS and with nonlinear finite element calculations. It is therefore difficult to assess the actual safety margin using these formulations.

### Acknowledgement

A special thanks goes to our colleagues S. Valsgård and G. Holtmark at DNV for their continuous support of the present work. Professor J. Helleland at the University of Oslo and professor J. Amdahl at NTNU has also been an important source of inspiration. Thanks also to DNV for sponsoring several internal R&D buckling and ultimate strength projects during the last years. Bjørn K. Haugland and Rolf-Ole Jensen at DNV are also saluted for their continuous backing of the present developments.

### References

- Byklum, E, and Amdahl, J (2002A). "Nonlinear buckling analysis and ultimate strength prediction of stiffened steel and aluminium panels". The Second Int. Conference on Advances in Structural Engineering and Mechanics, Busan, South Korea, 2002.
- Byklum, E, and Amdahl, J (2002B) "A simplified method for elastic large deflection analysis of plates and stiffened panels due to local buckling". Thin Walled structures, Vol. 40 (11), pp 923-951.
- Byklum, E (2002C). "Ultimate strength analysis of stiffened steel and aluminium panels using semi-analytical methods". Phd thesis, Norwegian University of Science and Technology, Trondheim, Norway.
- Byklum, E, Steen, E, and Amdahl, J (2004) "A semi-analytical model for global buckling and postbuckling analysis of stiffened panels". Thin Walled structures, Vol. 42 (5), pp 701-7171.
- Det Norske Veritas (2004). Rules for Classification of Ships.
- Germanischer Lloyd (2003). Construction Rules for Seagoing Ships.
- Hayward, R (2003). "Experimental and Theoretical Investigations Carried out by Germanischer Lloyd". Preliminary draft note.
- Marguerre, K. (1938). "Zur theorie der gekrümmten platte grosser formeändrug", Proceedings of the 5<sup>th</sup> international congress for applied mechanics, p. 93-101.
- Steen, E, Østvold, TK and Valsgård, S (2001). "A new design model for ultimate and buckling strength assessment of stiffened plates". PRADS 2001, Shanghai.
- Steen, E, Byklum, E and Vilming, KG (2004A). "PULS verification manual - PULS Version 2.0, May 2004". DNV Report No. 2003-0769, Rev.01.
- Steen, E, Byklum, E and Vilming KG(2004), "Computer Efficient Non-Linear Buckling Models for Capacity Assessments of Stiffened Panels Subjected to Combined Loads", ICTWS 2004, UK.